

Interpolation of Computerized Tomography Slices using 3D Digital Inpainting

Sandrerley R. Pires¹, Edna L. Flôres², Celia A. Z. Barcelos², Marcos A. Batista³

¹ Alves Faria Faculty, Goiânia, GO, Brazil

²Federal University of Uberlândia, Uberlândia, MG, Brazil

³Federal University of Goiás, Catalão, GO, Brazil

sandrer@alfa.br, edna@ufu.br, celiabz@ufu.br, marcos@catalao.ufg.br

Abstract

The visualization of image structures in 3D obtained from computerized tomography examinations aids the medical professional in the analysis of images and consequently, provides a more accurate diagnoses. As these images (slices) are spaced apart it becomes necessary to fill in the empty spaces to show the structure in 3D. The use of the virtual slice between the real slices following the restoration is a new approach to realizing slice interpolation aimed at 3D visualization. The goal of this article is to develop a method which produces a virtual slice with few empty regions and, through the use of an inpainting process using transportation and diffusion of information with a Partial Differential Equation, complete the virtual slices. The experimental results, presented by images 2D and 3D show the efficiency of the proposed method.

1. Introduction

The examination results of computerized tomography are usually printed on film or photographic paper. This allows any medical professional or even the patient to visualize the results of the examinations without the necessity of any additional resource. These results are represented on slices (image of one transversal cut of the examined structure).

The 3D visualization of computerized tomography examination results, that is, the visualization of the internal body structures as true to life, help the medical professional to be more accurate when analyzing examination results. The 3D visualization spares the medical professional the job of mental reconstruction of the human body's internal structure from the examination results, making the analysis process easier.

Between two consecutive real slices, there are usually spaces from 1.0 to 3.0 mm. It is necessary to fill in these empty spaces to show the structure in 3D, that is, to gener-

ate a 3D image. This process is called image interpolation. There are several methods for image interpolation in literature, like the Goshtasby et al. [10], Bors et al. [6] and the Wang et al. [18].

Traditional image interpolation methods are based on the goal of generating the virtual slices between the real slices from a computerized tomography examination. However, most of these methods [10, 6, 18] use only the information from two consecutive real slices to generate the virtual slice. This approach causes the incorrect curvature in the structure.

To solve the problems described above, the interpolation method of computerized tomography slices uses the following considerations:

- Gostasby and Turner [10] declare that between consecutive slices from computerized tomography examinations, there should not occur abrupt alterations of the tissues in the slices. The visual analysis of consecutive slices in Figure 1 permits visual verification.

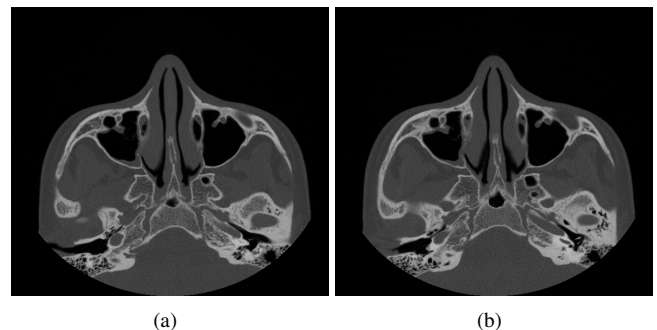


Figure 1. Images from two consecutive slices from a computerized tomography.

- Currently, there are several image restoration methods that recover damaged or occluded portions in an im-

age transferring the contours and texture from a neighborhood to internal areas to be restored. A method proposed by Bertalmio et al. [5] uses the image inpainting process through transportation and diffusion of information, Barcelos et al. [3] use the geodesic curves' information to promote the image inpainting.

As two consecutive computerized tomography slices are very similar and the restoration process can recover the well defined contours of damaged areas, this work proposes dividing the interpolation process into two steps. They are:

1. Obtaining the initial virtual slice;
2. Utilization of the image inpainting process.

The initial virtual slice must contain similar portions as those found in the two consecutive real slices. The non similar portions remain empty, that is, without usable information. This empty area must be filled in by an inpainting process applied to the image.

The fewer the empty regions in the initial virtual slice, the better the results of the image inpainting process will be. Thus, the goal of this work is:

1. To propose a method which obtains an initial virtual slice, where the slice empty area must be minimized by determination of the possible similarities between two consecutive real slices.
2. To propose a second method, based on the work of Bertalmio et al. [5], to realize image inpainting in a 3D image.

This article is based on a previous work that helped in the creation of the method proposed in this work, definitions of what is the initial virtual slice, modification of the method of Bertalmio et al. [5] to 3D image, as well as the presentation of the results obtained from the experiments and their analysis will be presented.

2. Previous Works

The method developed in this article uses some process already developed in previous works. They are:

- Goshtasby and Turner [10] proposed a linear interpolation process between the slices, where the similarity measurement between the pixel from a slice and its neighborhood in another slice defines the corresponding pixels. The connection between its pixels is the path to linear interpolation.

The method proposed in this article uses the same principles. However, a tolerance in comparison to the process of the pixels in real slices is created. Thus, it is possible that a resulting virtual slice has empty spaces when the comparison process fails, that is, the distance between pixels is greater than the tolerance.

- Wang et al. [18] proposed an approach where the free spaces between the slices were divided into a number of small cubes. From the analysis of the gray level found in the corners of these cubes, the direction of the interpolation process is defined. In this approach, the results are also similar to those obtained by linear interpolation.

The proposed method in this article also uses the pixels neighborhood, where the gray level which shows greater similarity in the neighbor real slice is the gray level chosen to defined the pixel in the interpolated slice.

- Bertalmio et al. [5] proposed an image inpainting process which is divided into two steps. The first step is the transportation of information, after this, the diffusion process is applied. Batista [4] propose a modification to the inpainting process. The diffusion step in the Batista approach is extended to the whole image, but outside of the inpainting area the diffusion process uses the edges conservation methods.

This work uses the approach proposed by Batista [4], but the domain of application is extended from 2D to 3D space.

All processes described above aim at producing the complete image interpolation. In this article, the goal is to obtain an initial virtual slice. With these slices it is possible to use the interpolation method that takes into consideration spaces in a wider context than only the space found between two consecutive slices.

This wider context can be obtained from transversal sections of the pixels' cube, when the cube is already complete, that is, with real and initial virtual slices. The use of inpainting in the transversal section naturally uses the wider context.

The use of the proposed transversal section in this method will allow the transportation of the contour information of several slices. The expected result is a correct reconstruction of the tissues.

The Goshtasby and Turner methods [10], Bors et al. [6] and Wang et al. [18] consider the hypothesis that no abrupt changes occur in tissue contours. Thus, they also consider the possible continuation of tissues in the pixel's neighborhood, the fundamental hypothesis of this work.

There are different ways of performing 3D reconstruction, such as the use of mesh, as in [17] and [7] or working on pixel's cube which is the procedure adopted in this work, as in [11].

3. Obtaining Initial Virtual Slice

The initial virtual slice contains the common portions from the two consecutive real slices. It is obtained by com-

paring all the areas of real slices, where the non similar regions contain empty values. These empty spaces must be filled in by some inpainting method.

The pixel by pixel comparison between two consecutive real slices can be a simple method for obtaining an initial virtual slice. When two pixels in the same position (x, y) , one in each slice, have the same gray level, then the virtual slices between them also have the same gray level. Figure 2 shows the results of this approach applied to the 23rd and 24th slices of a computerized tomography examination. The gray color indicates the pixels position whose values are not similar to the slice comparison process. The similarity perceived by visual analysis was not mapped by this process, as shown in Figure 2.

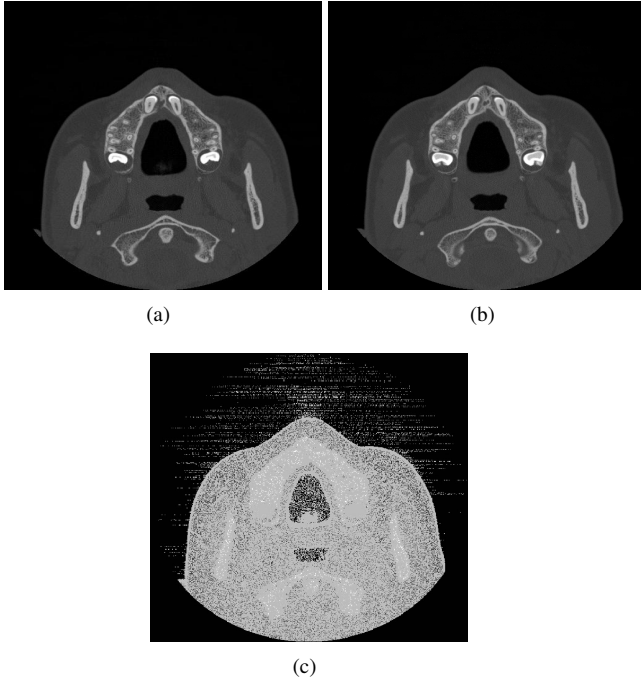


Figure 2. (a) and (b) two consecutive computerized tomography slices; (c) Similarity obtained in pixel by pixel comparison.

Table 1 shows the percentual numerical results obtained by comparison of three distinct slice pairs using the pixel by pixel comparison. The statistical correlation (c) [12, 8] was also calculated between the slice pairs as

$$c = \frac{\sum_{i=1}^m \sum_{j=1}^n (Ia_{ij} - \bar{Ia})(Ib_{ij} - \bar{Ib})}{\sqrt{(\sum_{i=1}^m \sum_{j=1}^n (Ia_{ij} - \bar{Ia})^2)(\sum_{i=1}^m \sum_{j=1}^n (Ib_{ij} - \bar{Ib})^2)}} \quad (1)$$

where:

- n, m indicate, respectively the number of lines and columns of the images;
- \bar{Ia} and \bar{Ib} indicate respectively the average intensity of the pixels in the images Ia and Ib ;
- Ia_{ij} and Ib_{ij} indicate respectively the intensity of the pixel (i, j) of Ia and Ib in this position.

Test	Slices	Similarity Pixel by Pixel	Statistical Correlation
1	3 and 4	40%	98.3%
2	23 and 24	44%	97.4%
3	51 and 52	42%	98.1%

Table 1. Results obtained by a comparison between the consecutive slices of three slice pairs in a pixel by pixel approach and by statistical correlation.

One observes in Table 1 that the statistical correlation between the slices expresses a much greater similarity from a visual analysis than similarity obtained from a pixel by pixel comparison. The statistical correlation shows that the similarity perceived by visual analysis is real. Thus, one concludes that to obtain an initial virtual slice which is to be restored in the second step of the process, a pixel by pixel comparison should not be used. A process based on statistical measurements must be used for obtaining the major possible similarity between slices.

3.1. The Proposed Method to Obtain an Initial Virtual Slice

In the pursuit of a method that produces an initial virtual slice with few empty regions, this work proposes the use of a standard deviation measure of the real slices involved in the process. The standard deviation indicates the average difference of gray levels between tissues contained in two consecutive real slices. Besides this, the proposed method uses a coefficient K that defines tolerance levels to the comparison process. The coefficient K can have values between 0 and 1 with the objective of reducing the tolerance, in the comparison process, obtained by the average of the standard deviation. If K has a value near 1, the tolerance

can be very high and an incorrect interpretation of the two different tissues as the same tissue. If K has a value near 0, the result can be the same as that of the pixel by pixel comparison.

The proposed method in this article aims at obtaining the initial virtual slice, and can be described by using the following steps:

1. Consider A and B as two real slices that will interpolate, generating between them the virtual slice C ;
2. From the slices A and B , one obtains the average from the standard deviation of the gray levels. By multiplying the results obtained by the tolerance coefficient K , the threshold Tg is obtained;
3. For each pixel C_{ij} to be interpolated in C , the distance between A_{ij} and B_{ij} is obtained, and between A_{ij} and the neighborhood pixels of B_{ij} ;
4. Repeat the same process between B_{ij} and A_{ij} , including the neighborhood pixels of A_{ij} ;
5. The minimal distance found in steps 3 and 4 is compared with Tg ;
6. If the least distance found in steps 3 and 4 is less than Tg , then there is information passed to the virtual slice C . The pixel C_{ij} will receive the value of A_{ij} if the lesser found distance is obtained in step 3, otherwise C_{ij} will receive the value of B_{ij} ;
7. If the minimal distance found in steps 3 and 4 is greater than Tg , then C_{ij} therefore it will receive an empty value.

4. The Digital Inpainting Algorithm

This article will use the algorithms proposed by Bertalmio et al. [5]. In his work, Bertalmio defines D as the image regions where the inpainting process will be applied. The region ∂D , which define the boundary of D , contains the information to be transported into the domain D . The process intercalates a step of information transportation from ∂D to D , following from a diffusion step.

4.1. Transportation

In this algorithm, the transportation of information to a point $P(x, y) \in D$ is realized through the use of a scalar product from normal vector \vec{N} at P with the vector \vec{s} that indicates the direction of the isochromatic line containing P . Figure 3 shows its vectors in the inpainting domain.

The normal \vec{N} is obtained calculating the gradient of laplacian in $P(x, y)$. The vector \vec{s} is the perpendicular vector defined by the gradient in $P(x, y)$.

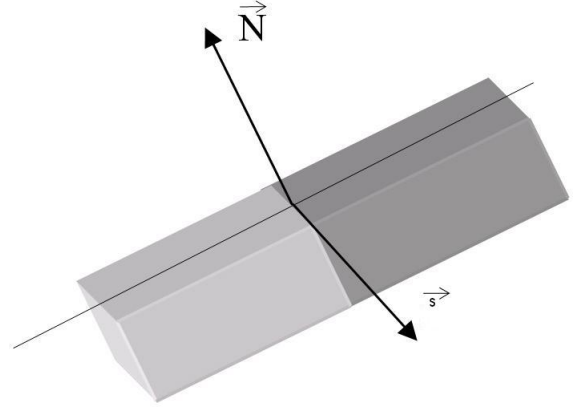


Figure 3. Shows a point $P \in D$ and the normal vector \vec{N} and isochromatic vector \vec{s} .

To obtain the vectors \vec{N} and \vec{s} at a point $P(x, y) \in D$ from image $I : R^2 \rightarrow R$, one can use the following expression:

$$\vec{N} = \nabla \mathcal{L}(I(x, y)),$$

where

$$\mathcal{L}(I(x, y)) = \Delta I(x, y) = \nabla(\nabla I(x, y))$$

and

$$\vec{s} = \nabla^\perp I(x, y).$$

Thus, the transportation step is obtained by

$$\frac{\partial I}{\partial t} = \nabla \mathcal{L}(I) \cdot \nabla^\perp I \quad (2)$$

where t is the time of the evolution in the transportation process. The transportation process is made only in the D domain.

4.2. Diffusion

The diffusion process, based on the mean curvature flow equation [16], has already been used in works such as [2, 9, 1]. The equation used in previous works is

$$I_t = |\nabla I| \operatorname{div} \left(\frac{\nabla I}{|\nabla I|} \right) \quad (3)$$

where:

$I(x, y)$ is the original image and $I(x, y, 0) = I(x, y)$.

Equation (3) realizes the diffusion in the orthogonal direction of the gradient.

Aiming to use Equation (3) and maintaining the image's edges, Malik and Perona [13], used Equation (3) with a edge detection process. The objective is to weaken the action of Equation (3) along the edge regions. The equation proposed by Malik and Perona is

$$I_t = \text{div}(g(|\nabla I|)\nabla I) \quad (4)$$

with $I(x, y, 0) = I(x, y)$.

In Equation (4) a G function is inserted. This function is non-increasing and obeys the following conditions:

- $g(0) = 1$;
- $g(s) \geq 0$, and;
- Se $g(s) \rightarrow 0$, when $s \rightarrow \infty$.

A new model inspired on the method proposed by Malik and Perona [13] was proposed by Barcelos et al. [3]. Its model is described in Equation (5):

$$u_t = g(|\nabla G_{\sigma} * u|) |\nabla u| \text{div} \left(\frac{\nabla u}{|\nabla u|} \right) - (1 - g(|\nabla G_{\sigma} * u|)) (u - I) \quad (5)$$

where “*” indicates the convolution between functions, and the initial condition is $u(x, 0) = I(x)$.

The model given by Equation 5, allows the diffusion of the image in the orthogonal direction of ∇u with speed $g(|\nabla G_{\sigma} * u|)K$, where $K = \text{div} \left(\frac{\nabla u}{|\nabla u|} \right)$. The chosen g function in this work is: $g(s) = \frac{1}{(1+s^2)}$.

5. The New Proposed Approach

With the goal of verifying the proposed method in this work, the image inpainting process proposed by Bertalmio et al. [5] and improved by Batista [4], needs to be increased from the 2D to the 3D domain.

Equation 2 was detailed for the 2D process in [4] and Equation 3 was detailed for the 2D process in [15]. In this work a 3D image is used, $u : \mathbf{R}^3 \rightarrow \mathbf{R}$, here $D \subset \mathbf{R}^3$.

The resulting 3D image of juxtaposition of real slices and initial virtual slice is an incomplete image. The empty regions of the initial virtual slice needs to be restored and this work proposes the 3D inpainting as a solution to the problem.

Thus, the inpainting process will be realized in a 3D domain. The empty spaces will be filled in through the use of a 3D process, where the considered context is greater than two slices. Following on, the new equations for 3D process are presented.

5.1. Transportation in 3D

The transportation step is obtained by Equation (2) presented in the previous section. Changing the 2D image, $I(x, y)$, to a 3D image, $u(x, y, z)$, one obtains:

$$\frac{\partial u}{\partial t} = \nabla \mathcal{L}(u) \cdot \nabla^\perp u \quad (6)$$

Detailing this equation:

$$\frac{\partial u}{\partial t} = \nabla \mathcal{L}(u) \cdot \nabla^\perp u = \nabla(\Delta u) \cdot \nabla^\perp u = \nabla(\text{div}(\nabla u)) \cdot (\nabla u)^\perp \quad (7)$$

After these developments, Equation (8) makes the transportation step into the new approach.

$$\begin{aligned} \frac{\partial u}{\partial t} = & - \left(\frac{\partial^3 u}{\partial x^2 \partial y} + \frac{\partial^3 u}{\partial y^3} + \frac{\partial^3 u}{\partial z^2 \partial y} \right) \cdot \left(\frac{\partial u}{\partial y} \right) + \\ & \left(\frac{\partial^3 u}{\partial x^2 \partial z} + \frac{\partial^3 u}{\partial y^2 \partial z} + \frac{\partial^3 u}{\partial z^3} \right) \cdot \left(\frac{\partial u}{\partial x} + \frac{\partial u}{\partial z} \right) - \\ & \left(\frac{\partial^3 u}{\partial x^3} + \frac{\partial^3 u}{\partial y^2 \partial x} + \frac{\partial^3 u}{\partial z^2 \partial x} \right) \cdot \left(\frac{\partial u}{\partial y} \right) \end{aligned} \quad (8)$$

5.2. Diffusion in 3D

The diffusion step is obtained by using Equation (5), considering $u : \mathbf{R}^3 \rightarrow \mathbf{R}$.

In this way, the diffusion term is given by:

$$\begin{aligned} & |\nabla u| \text{div} \left(\frac{\nabla u}{|\nabla u|} \right) = \\ & \frac{u_{xx}(u_y^2 + u_z^2) + u_{yx}(u_x^2 + u_z^2) + u_{zz}(u_x^2 + u_y^2)}{u_x^2 + u_y^2 + u_z^2} - \\ & \frac{2u_x u_y u_{xy} + 2u_x u_z u_{zx} + 2u_y u_z u_{yz}}{u_x^2 + u_y^2 + u_z^2} \end{aligned} \quad (9)$$

The g function used was: $g(s) = \frac{1}{(1+s^2)}$, with $s = K_g |\nabla u|$ as in the 2D process, where K_g is an attenuated coefficient.

6. The Implementation Process

The proposed Algorithm can be described as:

1. Create the 3D image with initial virtual slice:
 - Read all real slices of the examination;
 - Calculate how many virtual slices will be created;
 - Generate the initial virtual slices as explained in section 3.1;
 - Generate the 3D image through juxtaposition of real and initial virtual slices;
2. Read all necessary parameter to inpainting process. The parameters are:
 - M - the total number of iterations of the process;
 - Mt - the number of iterations of the transportation process;
 - Kt - the attenuation coefficient of the transportation step;

Md - the number of iterations of the diffusion process;

K_d - the attenuation coefficient of the diffusion step;

K_g - the attenuation coefficient of the g function;

3. Repeat M times

Repeat Mt Times

Transportation Process with Equation 8;

Repeat Md Times

Diffusion Process with Equation 9;

All routines were written in C++ and executed using a Pentium IV, 2.4Ghz computer, 1Gb of RAM and a video graphic card with 128Mb of memory. To show the 3D image an application also written in C++ and using the VTK library was used.

The execution time to reach an examination result with 52 real slices and 102 initial virtual slices is shown in Table 2.

Test	Process Step	Time (sec.)
1	Examination read	5
2	Initial virtual slice generation	17
3	3D Inpainting	550
4	Visualization	25

Table 2. The spent time for each step of the interpolation and visualization process.

After the execution of the first three steps, the user can execute the visualization step several times without the need to execute the first three steps again.

7. Obtained Results and Analysis

Figure 4 shows four consecutive slices. The first line, (a) and (b), are the real slices, and the second line, (c) and (d), the virtual slices after the 3D inpainting process. One observes that the process generates virtual slices with all the features of the real slices, but its also has specific features, which show the effectiveness of the proposed process. Also one observes the high quality of the virtual slices generated.

Figure 5 shows three images resulting from the 3D interpolation process proposed in this work. Two different transfer functions were used for the visualization process. The first function, Figure 5 (a) and (b), shows the human jaw bone in two positions and the second, Figure 5 (c), shows the human face using the same examination.

One observes that the proposed interpolation process produces a high quality 3D image.

Tests were carried out, which compared the proposed method to the Goshtasby et al. [10] and interpolation linear method. The visual result from one of these methods

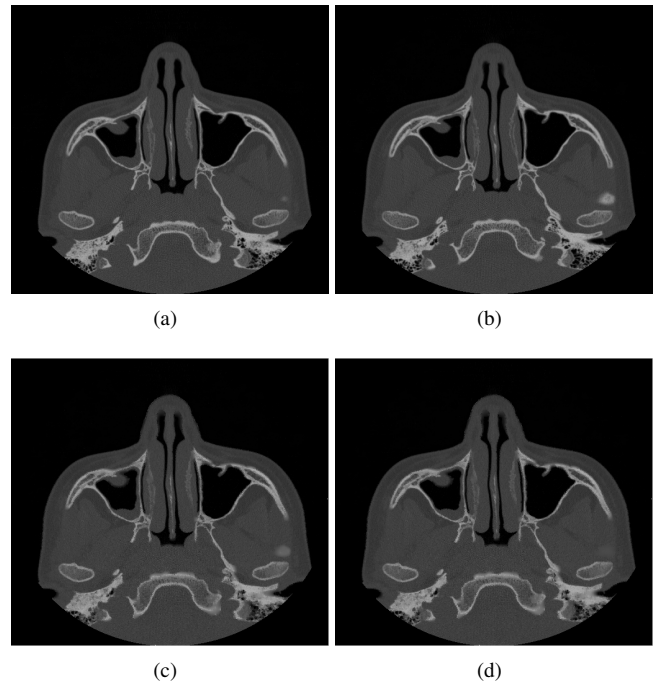


Figure 4. Output of the inpainting process to four consecutive slices. (a) and (b) real slices 43 and 44; (c) and (d) virtual slices 43.01 and 43.02.

can be seen in Figure 6. Two different points can be highlighted in the amplified results. The first in the upper central part, where the results obtained by the interpolation method, Figure 6 (c) and (d), and The Goshtasby et al. method, Figure 6 (e) and (f), present non-existent scarring to the image. The second, which easily shows in the center of the image, the formation of wrinkling which does not appear so apparent on the image of the proposed method, Figure 6 (a) and (b).

7.1. Conclusions

In terms of the method for obtaining the initial virtual slice and its restoration, it can be concluded that:

1. Obtaining the initial virtual slice allows for the use of the considerations made by Goshtasby et al. [10] and of the Bors et al. [6]. While these methods use these considerations to interpolate all slices, the method proposed in this work uses these considerations to obtain a initial virtual slice with empty spaces;
2. The use of statistical measurements in the comparison allows for the determination of an initial virtual slice with fewer and smaller empty regions;

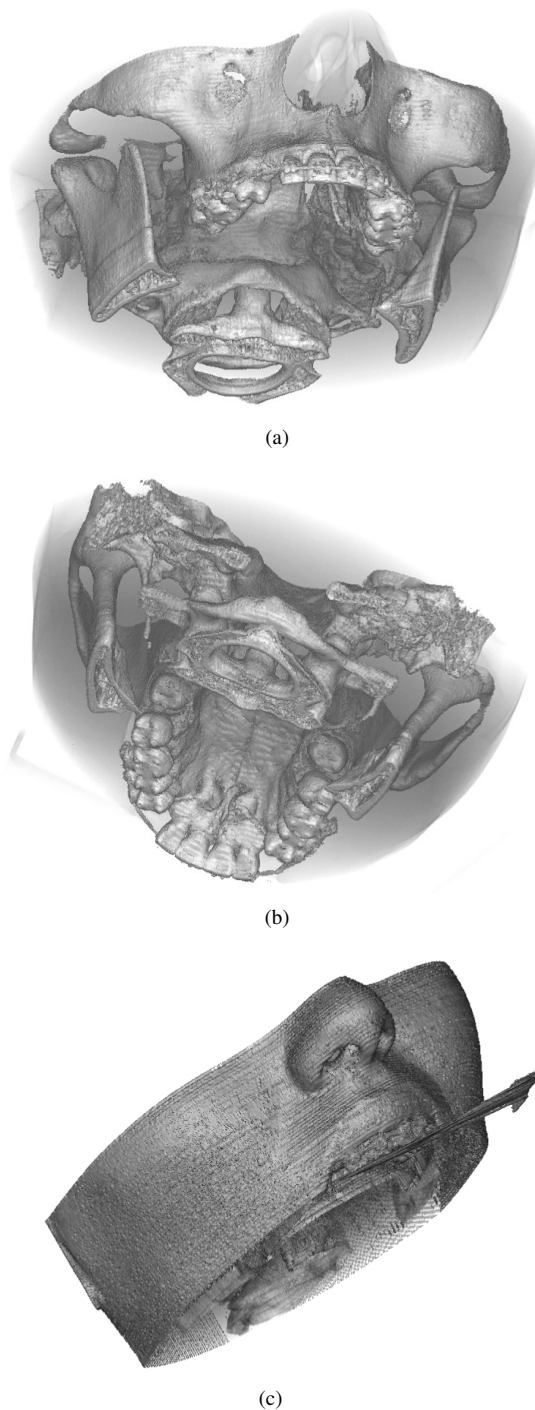


Figure 5. visualization of 3D image generated by proposed interpolation process. (a) and (b) human jaw bone. (c) human face.

3. The pixel by pixel comparison does not produce good

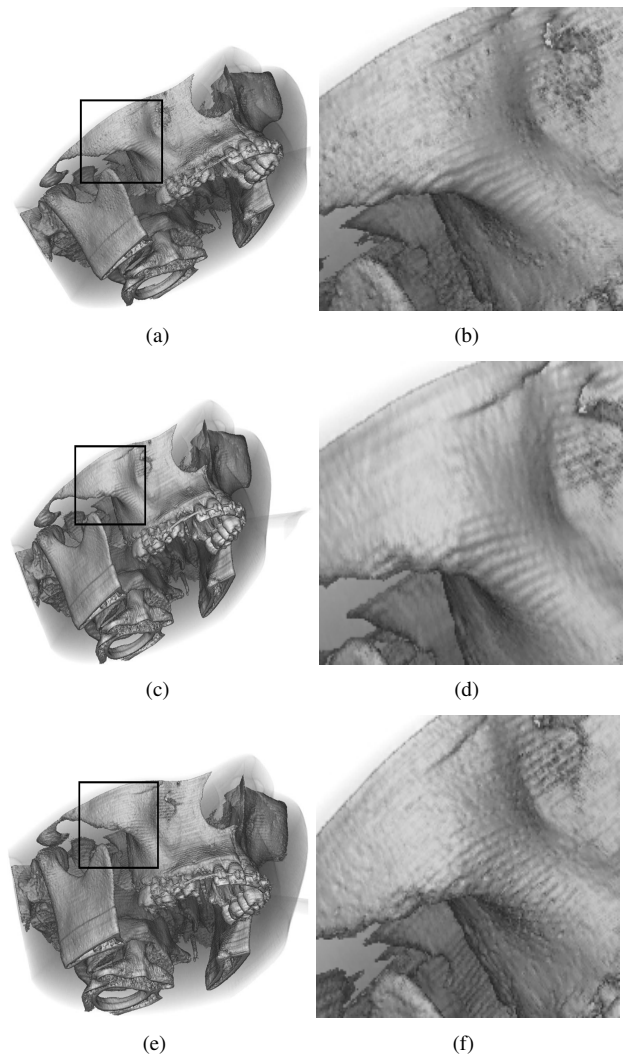


Figure 6. Obtained results from two interpolation methods and the proposed method. (a) Proposed method result. (c) Linear interpolation method result. (e) Goshtasby et al. method result.(b), (d) and (f) Amplified details of figures (a), (c) and (e) respectively.

results for obtaining an initial virtual slice;

4. The proposed method obtains an initial virtual slice with the same amount of filled in area and statistical correlation, showing the method's efficiency;
5. The improvement of the algorithm and equations from 2D to 3D shows the expected results, that is, a visible and sharp 3D image.
6. The 2D image generated by the proposed method obtained such high quality, it becomes difficult to recognize them as virtual slices;

One concludes that the proposed method allows one to obtain the initial virtual slice with small empty regions, making it easier to use than other proposed inpainting restoration methods.

The new approach in this work produced a 3D image with a high level of quality. Thus, the objective proposed was reached. The evolution of inpainting methods from 2D to 3D demonstrates to be a good approach, which can be used in other applications which use 3D images.

Some parameters, such as the transport coefficient and total iteration number, must be tested further as a few problems in 3D image diffusion can be observed in Figure 5.

Finally, one concludes that the proposed method presents a good result, by considering a context with several slices for the inpainting process thus, satisfying the purpose of this work.

7.2. Suggestion For Future Works

The method proposed in this article for obtaining an initial virtual slices shows better results than other methods that use the pixel by pixel comparison. However, it is possible to increase the quality of the results if the existing noise in the slices is removed before the application of the proposed method. Applying a smoothing process before obtaining initial virtual slices can reduce the noise on the slices, increasing the uniformity of the gray level intensity on the same piece of tissue.

Another suggestion is to change the method of 3D inpainting to the method proposed, to that of the proposed 2D image, by Martins [14]. The computational performance of their method is better than the method used in this work.

Acknowledgments

The author Celia A.Z. Barcelos is partially supported by a CNPq research grants.

References

- [1] M. Andrade. Um algoritmo iterativo para suavização e segmentação de imagens digitais. In *Anais do III Workshop em tratamento de Imagens, BH, MG, Brazil*, pages 11–20. June 2002.
- [2] C. Barcelos, M. Batista, A. Martins, and A. Nogueira. Level lines continuation based digital inpainting. In *Computer Graphics and Image Processing, XVII Brazilian Symposium on (SIBGRAPI'04)*, pages 50–57. October 2004.
- [3] C. Barcelos, M. Boaventura, and E. Silva Jr. A well-balanced flow equation for noise removal and edge detection. In *IEEE Transactions On Image Processing*, volume 12, pages 751–763. July 2003.
- [4] M. A. Batista. Retoque digital. Master's thesis, Universidade Federal de Uberlândia, Uberlândia, MG, Brasil, 2003.
- [5] M. Bertalmío, G. Sapiro, V. Caselles, and C. Ballester. Image inpainting. In *Proceedings of SIGGRAPH 2000, New Orleans, USA*, pages 417–424. July 2000.
- [6] A. G. Bors, L. Kechagias, and I. Pitas. Binary morphological shape-based interpolation applied to 3-d tooth reconstruction. In *IEEE Transactions on Medical Imaging*, volume 21, pages 100–108. February 2002.
- [7] P. Cateriano and L. Nonato. Vos: Volume on surface. In *Caderno de Computação - ICMC/USP*. 2003.
- [8] M. Degroot. *Probability and Statistic, Second Edition*. Addison-Wesley Publishing Company, 1989.
- [9] E. Galvanin, E. Silva, and J. Nogueira. Utilização de um modelo de equações diferenciais parcial no tratamento de imagens orbitais. July 2004.
- [10] A. Goshtasby, D. Turner, and L. Ackerman. Matching of tomographic slices for interpolation. In *IEEE Transaction on Medical Imaging*, volume 11, pages 507–516. December 1992.
- [11] G. Harald and O. S. Using the complex ginzburg-landau equation for digital inpainting in 2d and 3d. In *Scale Space Methods in Computer Vision*, number LNCS 2695, pages 225–236. 2003.
- [12] M. Hsieh and D. Tseng. Hiding digital watermarks using multiresolution wavelet transform. In *IEEE Transaction on Industrial Electronics*, volume 48, pages 875–882. October 2001.
- [13] J. Malik and P. Perona. Scale-space and edge detection using anisotropic diffusion. In *IEEE Transactions on Pattern Analysis and Machine Intelligence*, volume 12, pages 12–49. July 1988.
- [14] A. M. Martins. Retoque digital via linhas de nível. Master's thesis, Universidade Federal de Uberlândia, Uberlândia, MG, Brasil, 2003.
- [15] R. Oliveira and C. Barcelos. Morfologia matemática e equações de difusão em processamento de imagens. In *Relatório Técnico*. July 2004.
- [16] S. Osher and J. A. Sethian. Fronts propagating with curvature dependent speed: Algorithms based on hamilton-jacobi formulations. In *Journal of Computational Physics*, number 79, pages 12–49. 1988.
- [17] F. Taillardier and R. Deriche. Reconstruction of 3d linear primitives from multiples views for urban areas modelisation. In *Symposium on Photogrammetric Computer Vision - Graz*. September 2002.
- [18] Y. Wang, Z. Zhang, and B. Guo. 3d image interpolation based on directional coherence. In *IEEE Workshop on Mathematical Methods in Biomedical Image Analysis*, pages 195–202. December 2001.